

# Supporting Information

## **A broken tip allows a better trip: translocation of gold nanoparticles clusters through a nanopipette**

*Qianyi Wu, Jian Lv\*, Ruocan Qian\**

---

**Figures:**

**Figure S1.** *I-V* curves of intact-tip nanopipettes in a buffer solution at different times.

**Figure S2.** *I-V* curves of broken-tip nanopipettes in a buffer solution at different times.

**Figure S3.** High-resolution S 2p XPS spectrum of MPS-AuNPs. The low-binding-energy components were assigned to Au-S-R, where R was defined as  $-\text{CH}_2\text{CH}_2\text{CH}_2\text{SO}_3^-$ . The high-binding-energy components were assigned to  $\text{R}^1-\text{SO}_3^-$ , where  $\text{R}^1$  was defined as Au-S- $\text{CH}_2\text{CH}_2\text{CH}_2$ .

**Figure S4.** Stability of bare AuNPs and MPS-modified AuNPs in PBS. (a) Photographs of bare AuNPs before and after PBS addition. (b) Time-dependent UV-vis absorption spectra of AuNPs in PBS after incubation for 0, 1, 3, and 6 h. (c) Time-dependent UV-vis absorption spectra of MPS-modified AuNPs in PBS after incubation for 0, 1, 3, and 6 h.

**Figure S5.** Schematic of the experimental setup for the measurement of AuNPs blockade signals.

**Figure S6.** Current traces of MPS-modified AuNPs translocation through intact-tip nanopipettes at different voltages.

**Figure S7.** Current traces of MPS-modified AuNPs translocation through broken-tip nanopipettes at different voltages.

**Figure S8.** Current traces of translocation of MPS-modified AuNPs through intact-tip nanopipettes under pressure-assisted conditions at different voltages.

**Figure S9.** Dark-field imaging of MPS-AuNPs inside the broken-tip nanopipette during pressure application. (a) Representative dark-field image of a broken-tip nanopipette containing MPS-AuNPs. (b) Magnified view of the broken-tip region. The red arrows indicate larger and brighter scattering signals arising from local accumulation or aggregation of MPS-AuNPs.

**Figure S10.** Current traces of broken-tip nanopipettes filled with PBS buffer only under pressure-assisted conditions at 0 mV.

**Tables:**

**Table S1.** Rectification ratios of nanopipettes before and after tip breakage.

**Table S2.** Rectification ratios corresponding to the *I-V* curves corresponding to Figure S1&S2.

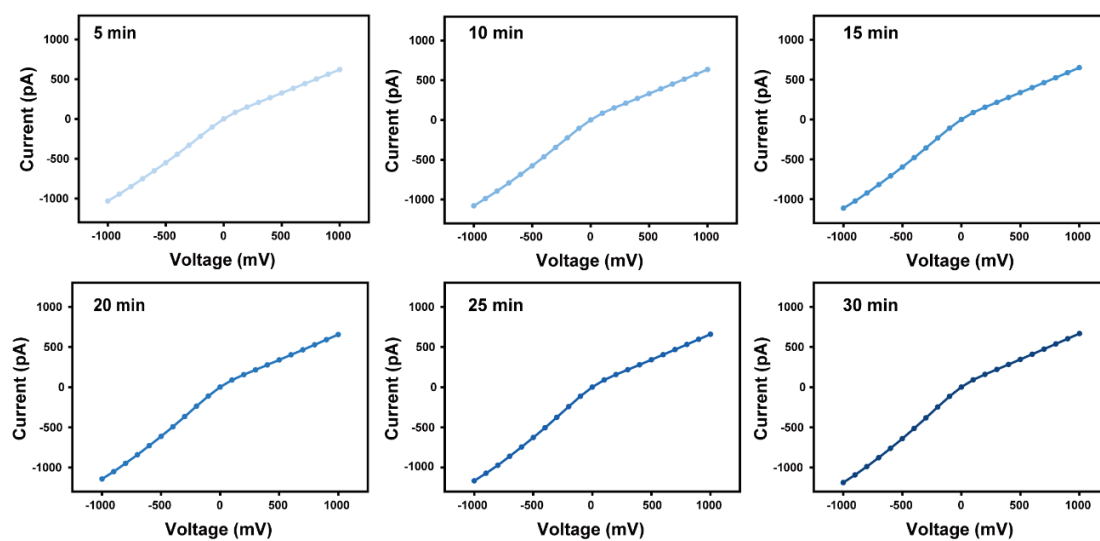


Figure S1. *I-V* curves of intact-tip nanopipettes in a buffer solution at different times.

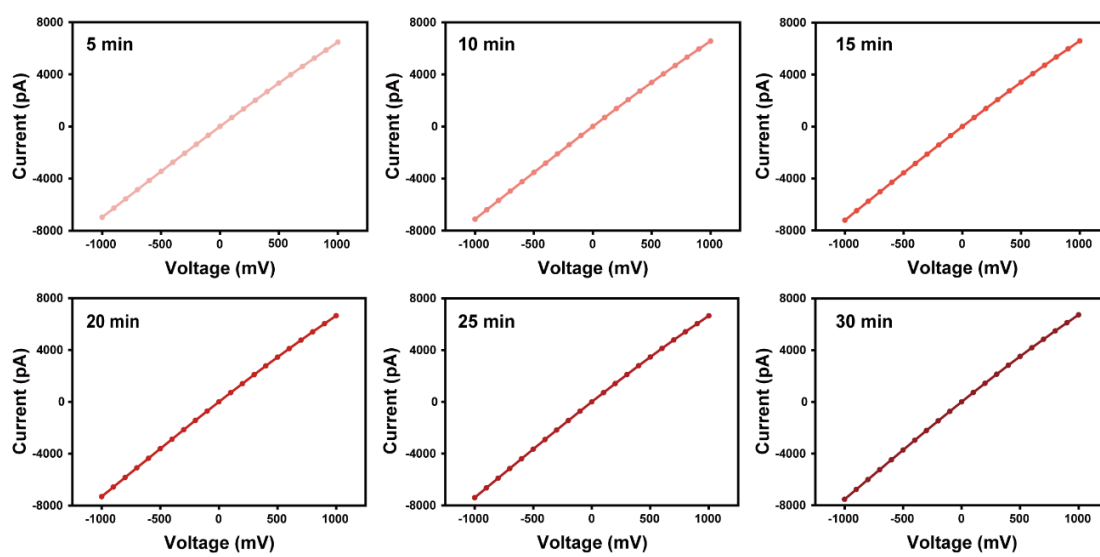


Figure S2.  $I$ - $V$  curves of broken-tip nanopipettes in a buffer solution at different times.

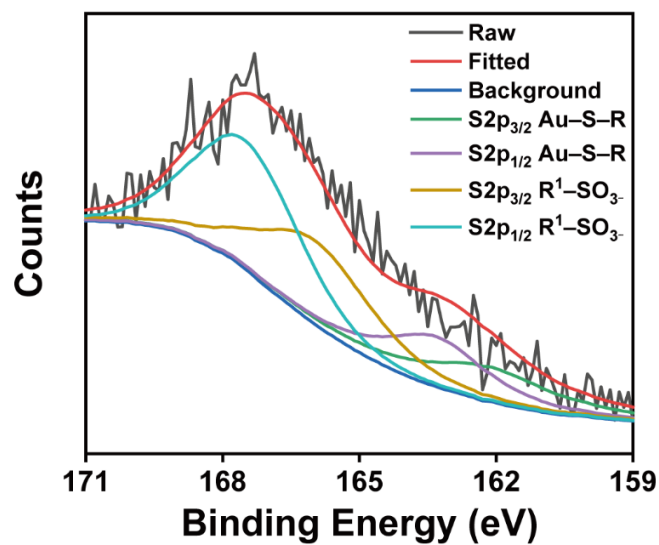


Figure S3. High-resolution S 2p XPS spectrum of MPS-AuNPs. The low-binding-energy components were assigned to Au-S-R, where R was defined as  $-\text{CH}_2\text{CH}_2\text{CH}_2\text{SO}_3^-$ . The high-binding-energy components were assigned to  $\text{R}^1-\text{SO}_3^-$ , where  $\text{R}^1$  was defined as  $\text{Au-S-CH}_2\text{CH}_2\text{CH}_2$ .

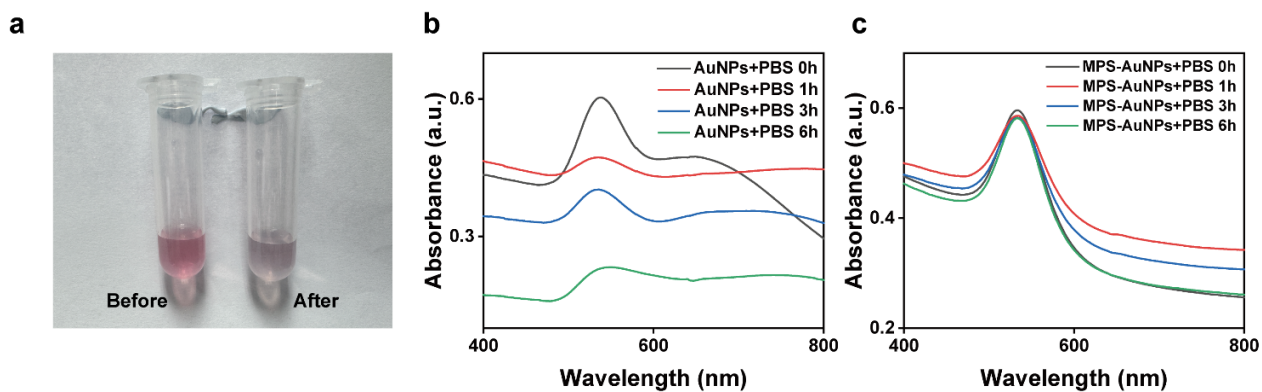


Figure S4. Stability of bare AuNPs and MPS-modified AuNPs in PBS. (a) Photographs of bare AuNPs before and after PBS addition. (b) Time-dependent UV-vis absorption spectra of AuNPs in PBS after incubation for 0, 1, 3, and 6 h. (c) Time-dependent UV-vis absorption spectra of MPS-modified AuNPs in PBS after incubation for 0, 1, 3, and 6 h.

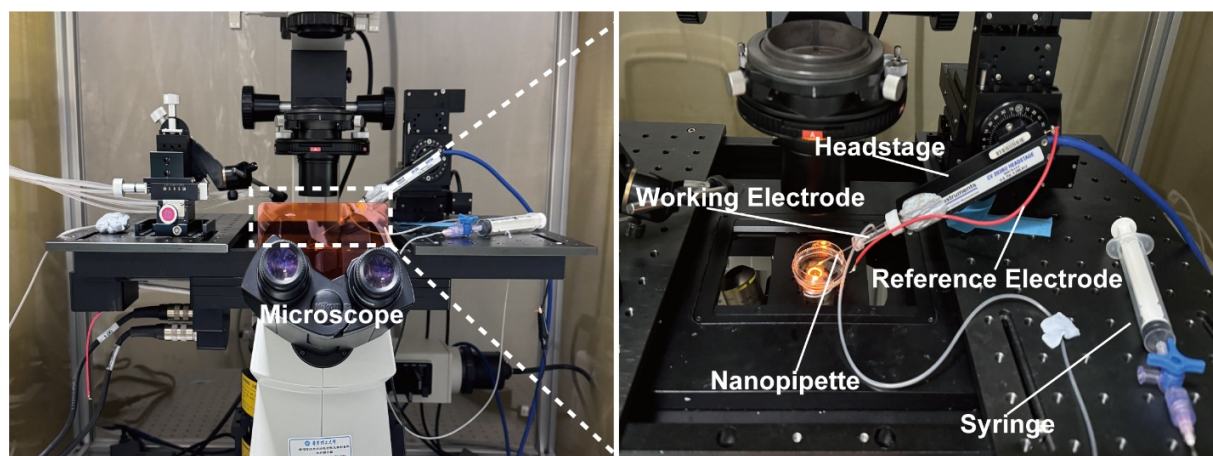


Figure S5. Schematic of the experimental setup for the measurement of MPS-modified AuNPs blockade signals.

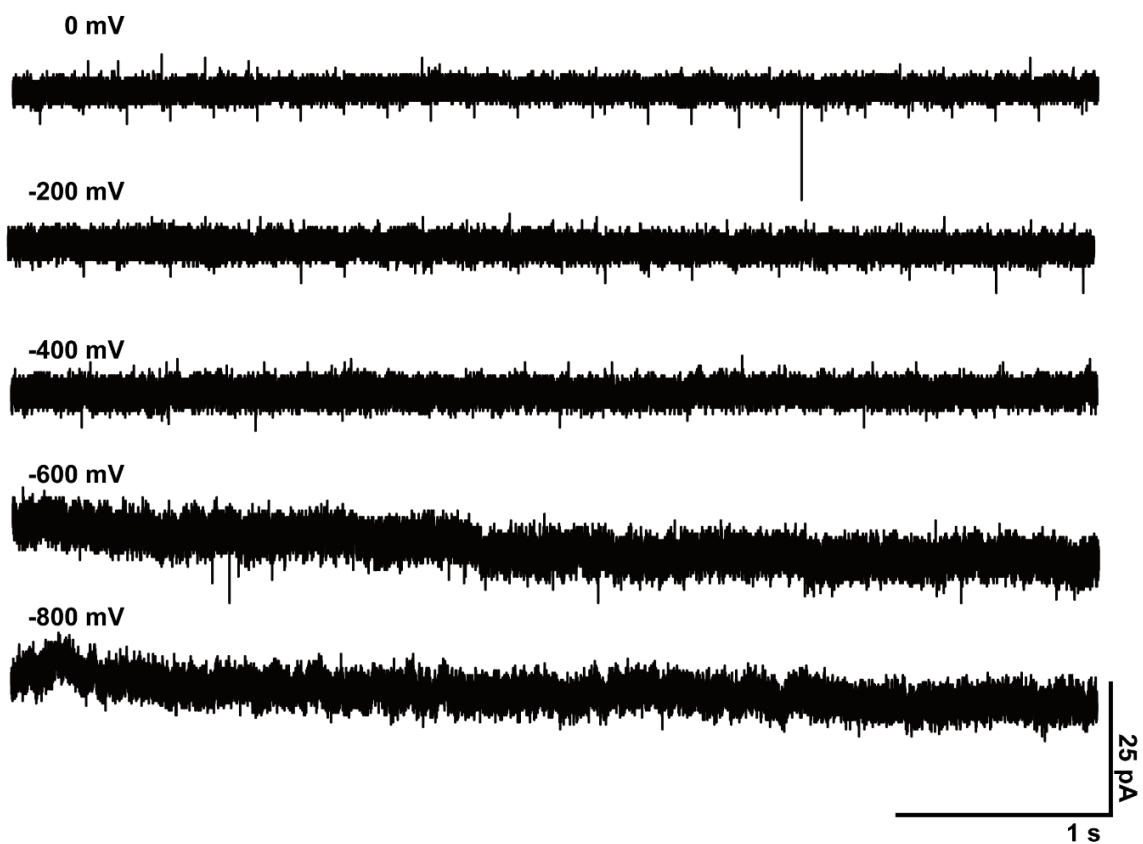


Figure S6. Current traces of MPS-modified AuNPs translocation through intact-tip nanopipettes at different voltages.

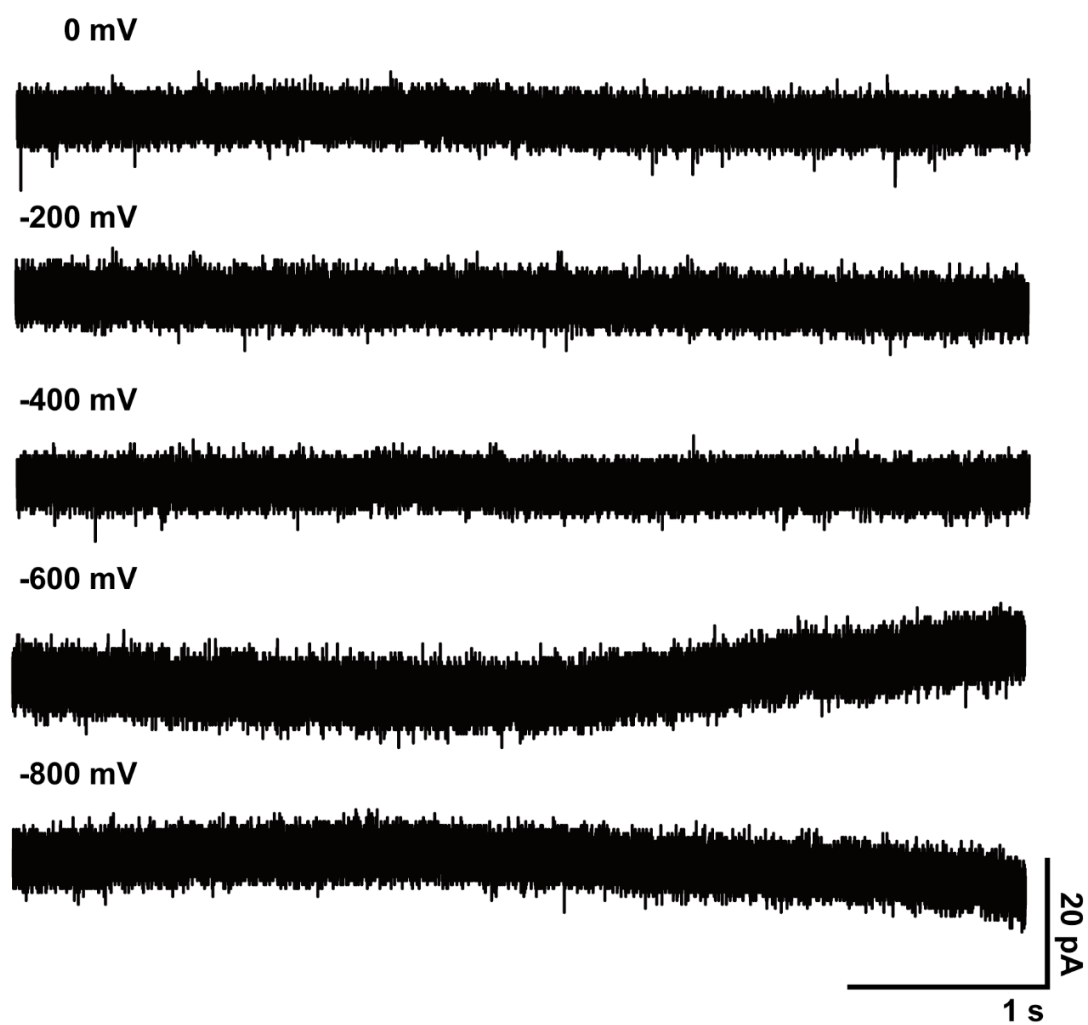


Figure S7. Current traces of MPS-modified AuNPs translocation through broken-tip nanopipettes at different voltages.

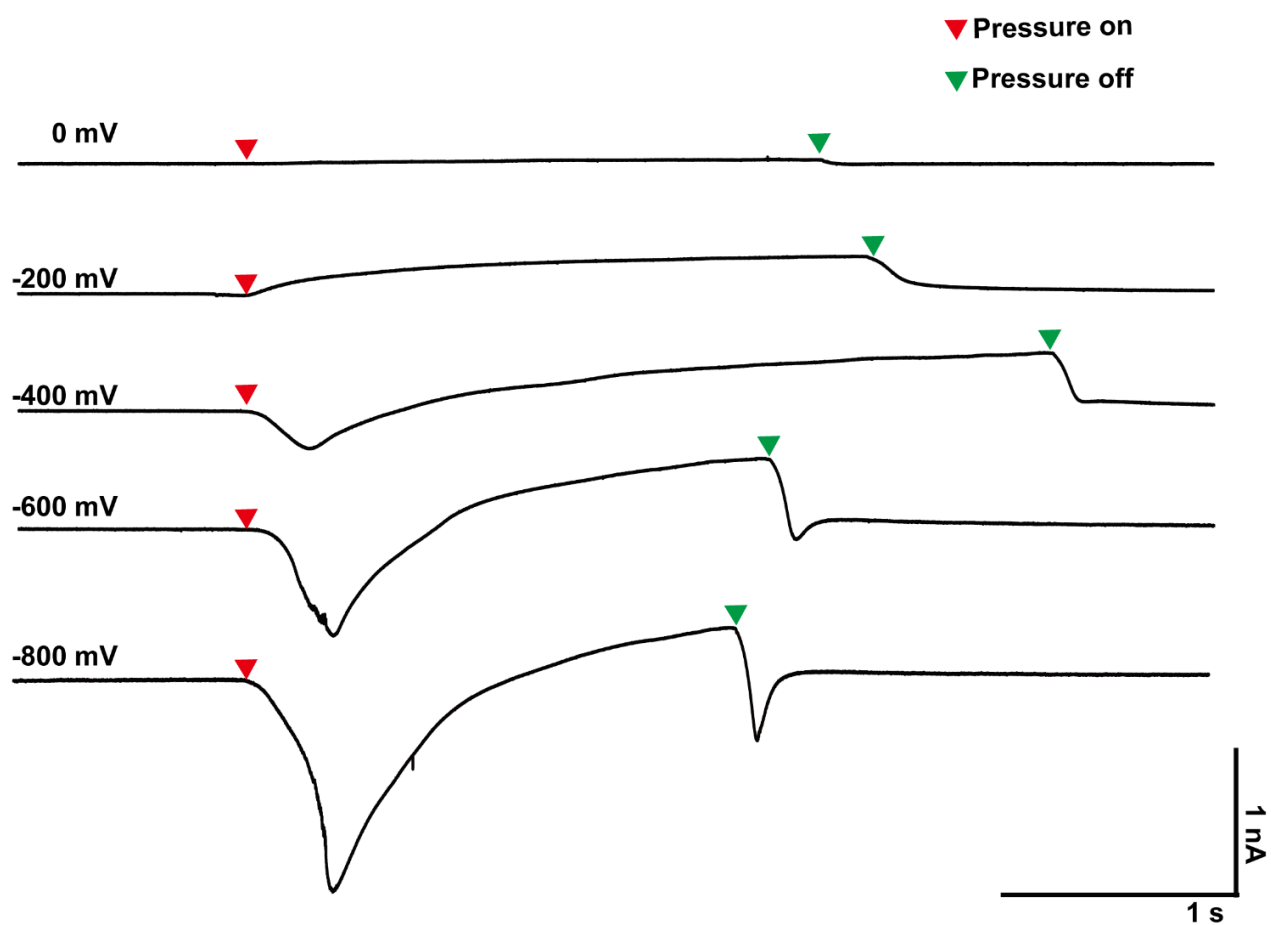


Figure S8. Current traces of translocation of MPS-modified AuNPs through intact-tip nanopipettes under pressure-assisted conditions at different voltages.

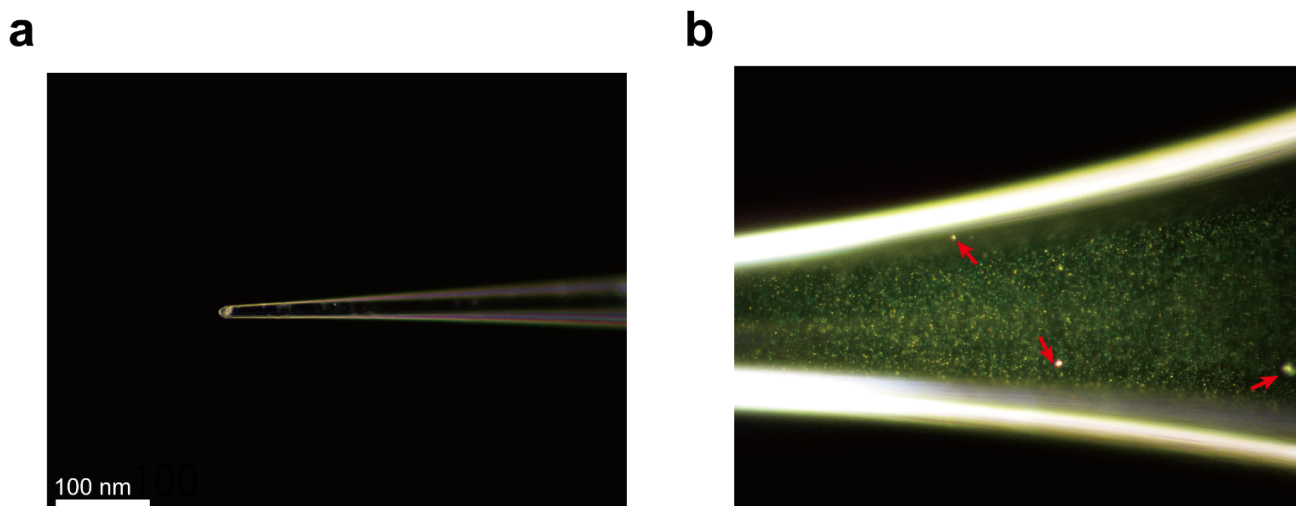


Figure S9. Dark-field imaging of MPS-AuNPs inside the broken-tip nanopipette during pressure application. (a) Representative dark-field image of a broken-tip nanopipette containing MPS-AuNPs. (b) Magnified view of the broken-tip region. The red arrows indicate larger and brighter scattering signals arising from local accumulation or aggregation of MPS-AuNPs.

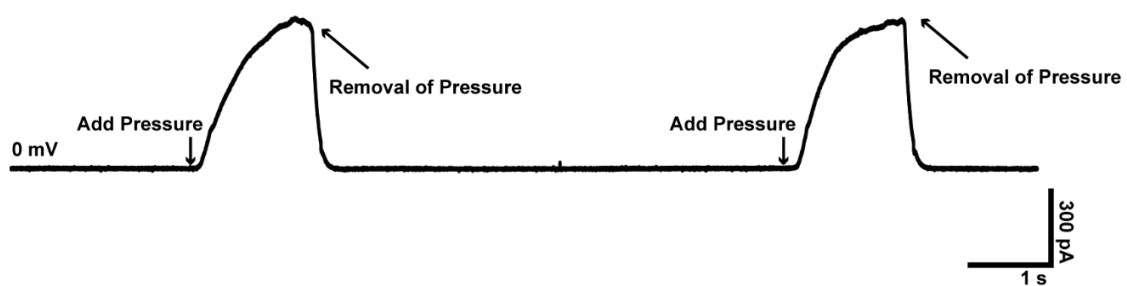


Figure S10. Current traces of broken-tip nanopipettes filled with PBS buffer only under pressure-assisted conditions at 0 mV.

Table S1. Rectification ratios of nanopipettes before and after tip breakage.

Rectification ratio (intact-tip nanopipette)	Rectification ratio (broken-tip nanopipette)
1.58	1.07

Table S2. Rectification ratios corresponding to the  $I$ - $V$  curves corresponding to Figure S1&S2

Time (min)	Rectification ratio (intact-tip nanopipette)	Rectification ratio (broken-tip nanopipette)
5	1.66	1.07
10	1.70	1.08
15	1.71	1.09
20	1.74	1.10
25	1.77	1.11
30	1.78	1.11